

Power quality disturbance mitigation in grid connected photovoltaic distributed generation with plug-in hybrid electric vehicle

Basaralu Nagasiddalingaiah Harish, Usha Surendra

Department of Electrical and Electronics Engineering, School of Engineering and Technology, CHRIST (Deemed to be University), Bangalore, India

Article Info

Article history:

Received Sep 4, 2022

Revised Apr 22, 2023

Accepted Apr 24, 2023

Keywords:

Direct quadrature control
Multicarrier space vector pulse width modulation
Photovoltaic generator
Plug-in electric vehicle
Total harmonic distortion

ABSTRACT

In the last twenty years, electric vehicles have gained significant popularity in domestic transportation. The introduction of fast charging technology forecasts increased the use of plug-in hybrid electric vehicle and electric vehicles (PHEVs). Reduced total harmonic distortion (THD) is essential for a distributed power generation system during the electric vehicle (EV) power penetration. This paper develops a combined controller for synchronizing photovoltaic (PV) to the grid and bidirectional power transfer between EVs and the grid. With grid synchronization of PV power generation, this paper uses two control loops. One controls EV battery charging and the other mitigates power quality disturbances. On the grid connected converter, a multicarrier space vector pulse width modulation approach (12-switch, three-phase inverter) is used to mitigate power quality disturbances. A Simulink model for the PV-EV-grid setup has been developed, for evaluating voltage and current THD percentages under linear and non-linear and PHEV load conditions and finding that the THD values are well within the IEEE 519 standards.

This is an open access article under the [CC BY-SA](https://creativecommons.org/licenses/by-sa/4.0/) license.



Corresponding Author:

Basaralu Nagasiddalingaiah Harish

Department of Electrical and Electronics Engineering, School of Engineering and Technology, CHRIST (Deemed to be University)

Bangalore, India

Email: bn.harish@res.christuniversity.in

1. INTRODUCTION

Electric vehicles (EVs) connected to the electrical grid may cause transformer overload, harmonics, and voltage imbalance. EV penetration changes voltage profile abruptly, when numerous residences install 1.6 kW EV chargers connected to the distribution system [1]. Residential EV charging would need large loads on lower side voltage distribution networks. EVs' energy needs may impact the distribution network [1], [2]. A strategy to mitigate the power quality of the EVs' intermittent connections to the PV bus is essential. The smart charging strategy for plug-in hybrid electric vehicles (PHEV) in distribution power generation is to use a hybrid planning method (HPM) which is suitable for evaluation of the cost benefits. The smart charging control technique uses an integrated strategy incorporating both the vehicle-to-grid (V2G) and the grid-to-vehicle (G2V) charging architecture [2].

PHEV charging using household PV systems and low voltage quality issues are also discussed. The reactive power injection comes from the bus voltage difference. Therefore, a solution integrating PV active power curtailment to alleviate voltage imbalance and voltage quality concerns is necessary while using battery energy management. One of the two consensus algorithms, in\$, takes advantage of the plug-in electric vehicle

(PEV) battery's restricted storage capacity and security operation center (SOC) [3]. Sharing the drop in real PV power during overvoltage is another consensus. The literature's method compensates for overloading caused by reverse power flow and voltage sag caused by a higher load. To maximize power efficiency in the distribution network, the algorithm coordinates PEV battery charging and discharging. PV source active power curtailment is reduced through charge synchronization. To maximize power efficiency in the distribution network, the algorithm coordinates PEV battery charging and discharging. Charging coordination reduces active power curtailment from PV sources. A four-wire three phase system and a PV source are used for this study.

Despite its stochastic nature, energy storage systems (ESS) allow control approaches to effectively employ power from renewable energy sources (RES). While EV charging and discharging are adopted, this ESS is riding a new function. Controlling active and reactive power keeps the grid's power factor at unity. In [4] 5,000 EVs connected on a 33 bus system with reactive power control. EVs may be deployed in greater numbers while retaining a unity power factor, according to the analysis. EVs may be charged at varied voltage levels at any distribution network point using a fuzzy-based controller with decentralized coordination. At the EV's connecting point, conveying charging time, energy requirements, and voltage costs money. Due to an unscheduled surge in electric vehicle charging, the distribution network's peak load would climb, enhancing electricity quality [5]. The variation of topology in the onboard chargers shows that the filter size, current triple, switch stress and voltage ripple are all reduced. The purpose is to measure the power quality indices at the source, which depends on the total harmonic distortion (THD) and the power factor. The three-level direct current to direct current (DC-DC) converter is part of the onboard charger topology, and it receives its DC input from a regulated rectifier in the power system. This implementation is preferable to other topologies because of the smaller size of the filter elements [6].

PFC-based bridgeless Cuk converters improve charge efficiency. Standards reduce THD, and the power quality index improves power quality. It charges efficiently [7]. EV-connected distributed systems correct PFC with an interleaved Landsman converter. Output voltage harmonics decrease input current harmonics. Constant current and voltage charging maintain current control [8]. Power quality and grid power flow in the PV array-connected system are investigated [9]. The controller regulates voltage, power factor, and neutral power. The controller also regulates power quality actively [10]. PV capacity and grid placement effect voltage fluctuations. Light flickers may persist as EV use rises. The approach improves voltage profile during fluctuation transients [11].

The publication combines shunt active power filter and grid-connected PV generation. The unified system provides reactive power correction, current harmonics, and active power with good irradiation. It acts as a shunt active power filter under low light. PV generation, harmonics suppression, and reactive power adjustment are achieved with massive storage batteries [12]. Reduction of voltage unbalance factor (VUF) by appropriately choosing charging/discharging state in all three phases and power rating of PEVs is the article's contribution. Three scenarios, first without PEVs, the second scenario with the coordinated, and the third scenario in the uncoordinated charging, applied for voltage unbalance factor (VUF) reduction [13]. The household loads, actual grid, EV loads and PV power production, are detailed [14]. DC charger using adaptive control approach show how basic PV/charger functionalities and tolerance to fluctuating solar irradiation are achieved [15]. A two-stage battery charger with a sinusoidal pulse width modulation (SPWM)-controlled AC-DC stage and a predictive duty cycle-controlled DC-DC stage. Predictive control absorbs DC bias from transformer current by adjusting peak amplitude value, allowing quick battery current management [16]. Three-level bidirectional converters have smaller filter inductors than ordinary DC-DC converters. Switch voltage stress is half the input dc link voltage. Weak feeder radial distribution systems experience undervoltage. EVs, heat pumps, home loads, and remote faults can lower voltage. Transformers in low-voltage distribution grids contain only off-load tap-changers, therefore a high-voltage voltage drop may extend to the reduced voltage side [17].

Measuring the criteria that determine power quality problems in distribution networks owing to EV penetration requires higher technical competence. The distribution network's harmonic component is measured via field measurements. While PV generators are penetrated in the grid that supplies the EVs the power quality issues are reduced using the power converter. A single power converter is used to get rid of power factor correction, neutral current compensation, harmonic elimination and voltage regulation using the bidirectional power in the batteries in the EVs and power sync between the grid and the EVs. Optimal usage of power electronic converters aids in good power quality maintenance in the grid structure. The distribution system voltage profile changes as EVs connect. Single-phase onboard charging ranges from 1 kW at residences to almost tens of kW for DC level 2 rapid charging [18]. However, due to their energy demand, EVs may cause power usage peaks and other power quality issues [19], [20]. In PV power generation plant, power quality improvement involves charging batteries during low demand and discharging during high demand. Power that is capable of being connected to the power plant without affecting power quality is called hosting capacity.

Literature incorporates dispersed generation into the power system via hosting capacity. Intelligent process-based electrical charging is developed using the data mining approach for EVs with driver assist application. Coordination of V2G with the PV integration [21]. About the circuit available for vehicle charging is explained in [22]. Power quality in the power system due to an electric vehicle is discussed in [23]. Under smart grid environment usage of plugin electric vehicles is explained in [24]. The bidirectional operation of the electric vehicle battery is explained in [25]. In a residential area charging an electric vehicle is discussed in [26]. In a distributed solar power generation charging a battery is explained in [27]. A detailed literature survey of electric vehicle transportation is given in [28]. Charger in a local smart grid battery with the vehicle is detailed in [29]. The grid-connected residential land plug-in hybrid electric vehicle (PHEV) concept is explained in [30]. Power quality management in a PV which is supplying to grid is explained in [31].

The design of various converters and the power quality of those converters are detailed in [32]. Time and frequency analyses are carried out in [33]. A bidirectional onboard charger is explained in [34]. Other articles on power quality with PV power generation is given in [35]–[40] PV system with EV and battery charging is discussed in [41]–[43]. In this paper, a three-level inverter with multicarrier space vector pulse width modulation (SVPWM) is explained for power quality issues. The PV power generation is integrated to this inverter for transfer the power to the grid. MATLAB is used to carry out the experimentation of various cases. Introducing DQ based composed controlled inverter to check the performance of the power quality improved is discussed in detail in the following sections. A bidirectional converter for the charge control of the EVs batteries along with the constant current loop forms the first controller. At the same time, the PV integration to the grid and the power quality disturbance mitigations form another loop with three-level inverters. DQ control and multicarrier SVPWM controller aides in the overall power quality disturbance mitigation. Synchronization of PV power generator with the distribution system maintains the 440 V/50 Hz specification at the point of common coupling (PCC). MATLAB simulation reduces power quality disruption caused by EV penetration in the distribution system. A satisfactory level of THD and power factor is observed in the grid connected PV distributed generation with PHEV. THD and power factor obtained from DQ controlled multicarrier SVPWM method is found to be better than that of the $I\cos\phi$ implementation. This implementation is best suited for smart building applications since bidirectional operation is adopted. Section 2 explains methodology, section 3 discusses on results; followed by section 4 explain conclusion and references.

2. THE PROPOSED METHOD

2.1. Power quality disturbance mitigation using DQ controller and bidirectional charger

The power flow illustration of the implementation is shown in Figure 1. Power flow from the Battery is considered to be bidirectional, while the power from the PV is considered as unidirectional. Grid has bidirectional power flow since the inverter is tied to grid. PV surplus power must be supplied to the grid.

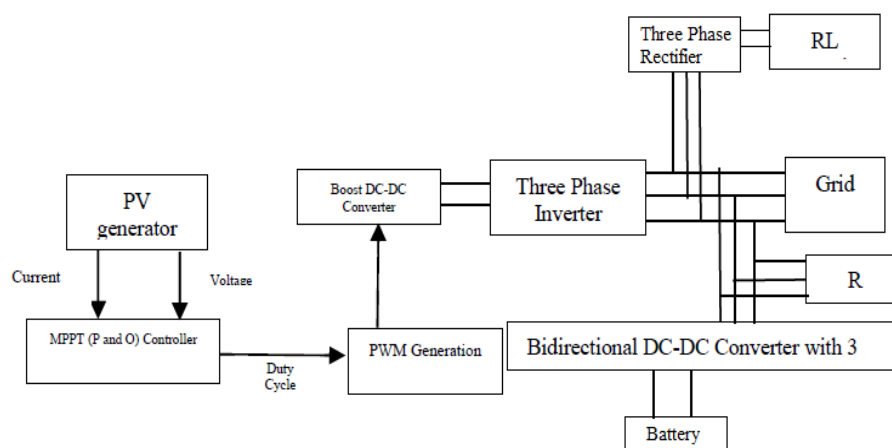


Figure 1. Power flow diagram in the proposed implementation

Mitigation of power quality disturbance while EV connection in the distributed generator PV interfaced distribution system involves two controllers, one for the grid interfacing and another for the bidirectional operation of the battery charger. Both controllers combine to act as the power quality disturbance

mitigation configuration. The complete configuration of the power quality disturbance mitigation is depicted in Figure 2.

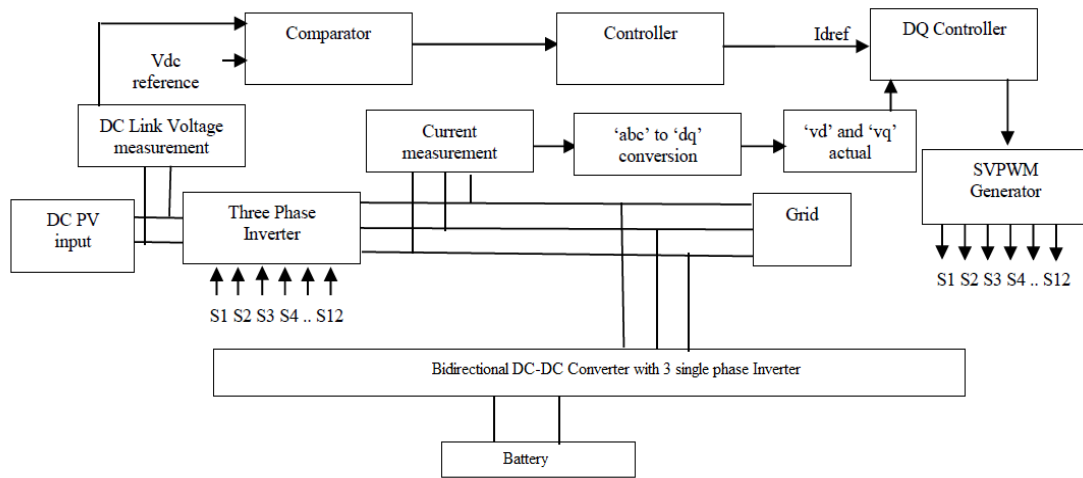


Figure 2. Control flow diagram in the proposed implementation

The perturb and observe algorithm for maximum power point tracking (MPPT) tracks maximum power from PV integrated with the grid. The proposed implementation develops the mitigation in grid connected PV distributed generation with PHEV by merging the battery's constant current charging loop, the grid synchronization loop, and a power quality disturbance mitigation loop. The PV is connected to a boost converter, as shown in Figure 2, and the boost converter is regulated by an MPPT control feed-forward loop, which generates pulses to the DC-DC converter following MPPT. DC-DC converter output connected to DC link supplies a grid integrated three-level inverter controlled by multicarrier SVPWM. EV, linear/non-linear load combinations are connected. The inverter has to take care of the power quality problems created by these loads. Current and voltage from the inverter output are decoupled to obtain the synchronous reference frame components. Decoupled components from the voltage and current response are used to find the reactive and real power. Instantaneous reactive and real power is the point from where the droop controller starts. The overall control configuration of the DQ-controlled PV-EV-grid topology is given in Figure 2. As shown in (1) and (2) defines the real and reactive power from the decoupled current and voltage components of inverter output.

$$p = \frac{3}{2}(V_{od}i_{od} + V_{oq}i_{oq}) \quad (1)$$

$$q = \frac{3}{2}(V_{oq}i_{od} - V_{od}i_{oq}) \quad (2)$$

Since the instantaneous real and reactive power is noisy. Corner frequency ω_c with low pass filter is applied as given in (3) and (4).

$$P = \frac{\omega_c}{s + \omega_c} p = -P\omega_c + 1.5\omega_c(v_{od}i_{od} + v_{oq}i_{oq}) \quad (3)$$

$$Q = \frac{\omega_c}{s + \omega_c} q = -Q\omega_c + 1.5\omega_c(v_{oq}i_{od} - v_{od}i_{oq}) \quad (4)$$

2.2. Phase locked loop (PLL)

The instantaneous phase angle of the inverter output that acts as the reference for the inverter is generated from the PLL. Generation of reference phase angle is as shown in Figure 3. Similar to real and reactive power direct axis voltage V_{od} is filtered using the low pass filter to obtain V_{odf} . As shown in (6) defines the relation as shown in Figure 3.

$$V_{odf} = \omega_{cPLL}(V_{od} - V_{odf}) \quad (5)$$

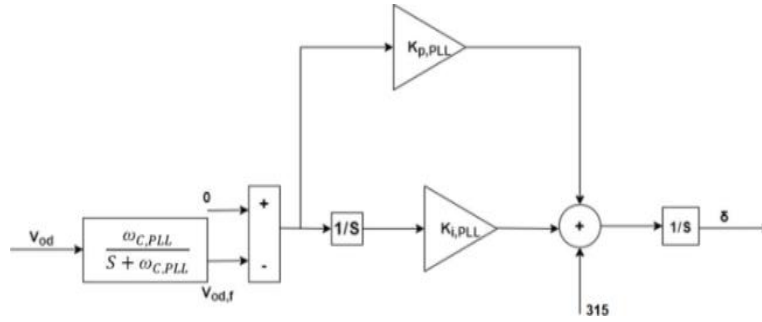


Figure 3. PLL module

2.3. Voltage controller

Voltage and frequency generated from the droop characteristics is got for the voltage regulation as shown in Figure 4(a) shows the quadrature current reference generation and Figure 4(b) shows the direct axis reference generation. The proportional integral (PI) controllers that generate the current reference from the voltage and the phase components are developed in the voltage controller for further controlling the inverters. The state equation of the voltage controller is given below in (6) and (7).

$$\Phi'_d = \omega_{cPLL} - \omega^*; i_{ld}^* = k_{iv,d}\Phi_d + k_{pv,d}\Phi'_d \tag{6}$$

$$\Phi'_q = v_{oq}^* - v_{oq}; i_{lq}^* = k_{iv,q}\Phi_q + k_{pv,q}\Phi'_q \tag{7}$$

where Φ'_d is the angular rad/sec difference with the reference, Φ'_q is the voltage difference with the reference.

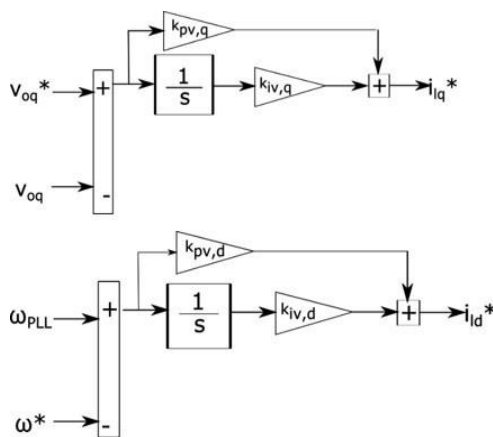


Figure 4. Voltage controller (a) q axis current reference and (b) d axis current reference

2.4. Current controller

The current controller compares the direct and quadrature axis current obtained at the inverter output to the voltage controller reference. The reference voltage is given to the SVPWM for the inverter Figure 5. The current controller outputs the reference d- and q-axis voltages from (8) and (9).

$$v_{id}^* = -\omega_{cPLL_n} L_f i_{lq} + k_{ic,d} \Sigma(i_{ld}^* - i_{ld}) + k_{pc,d} \Sigma(i_{ld}^* - i_{ld}) \tag{8}$$

$$v_{iq}^* = -\omega_{cPLL_n} L_f i_{ld} + k_{ic,q} \Sigma(i_{lq}^* - i_{lq}) + k_{pc,q} \Sigma(i_{lq}^* - i_{lq}) \tag{9}$$

where V_d are I_d are controlled d -axis V and I , V_q , and I_q controller q -axis V and I , R -grid side resistance, L -grid side inductance. The V_{dq} calculation is converted to V_{abc} . Reference V_{abc} thus generated is compared with the actual V_{abc} to get modulated in the pulse width modulation. PHEV load is configured as given in the following section.

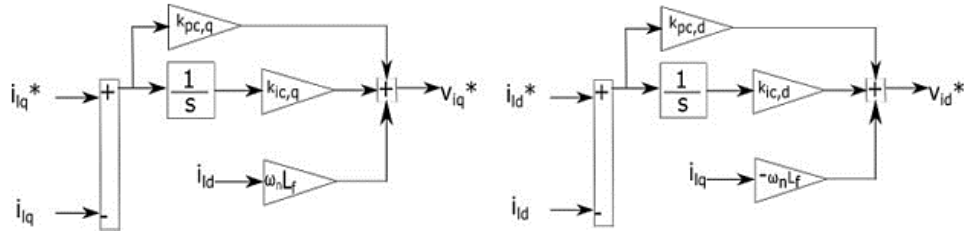


Figure 5. Current controller

2.5. PHEV configuration

PHEV configuration is synonymous to the battery setup. Bidirectional power transfer between the PCC and the battery and vice versa defines the PHEV configuration. The current control loop for the charging application is depicted in Figure 6. According to the control loop, the constant current is maintained for charging the EV battery. The reference current of the I battery is set to maintain a constant charging current for the EV’s battery. PI controller is used to obtain a better output from the charger for efficiently charging the EV’s battery. The PHEV charger is a constant current charger. The charger current is set as the set point the current from the battery is measured. The compared current is error current. The error current is given to the PI controller. The PI controller calculates the duty cycle. The duty cycle is passed to pulse-width modulation (PWM) generator to generate the pulses to control the current from the battery. There are two switches. M1 is the buck switch and M2 is the boost switch. The M1 is operated for charging the battery and M2 is operated for discharging the battery to grid. Here the charger is in single phase where each phase has one circuit.

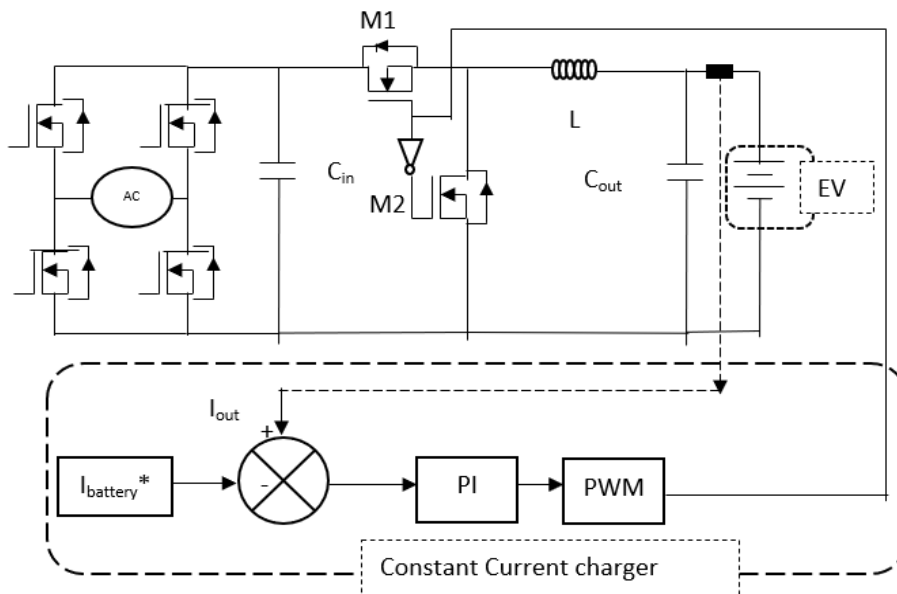


Figure 6. Bidirectional DC-DC converter control

Linear/non-linear load modifies current flow in both the direction DC-DC converter in the distribution system with EV. Power system load changes activate PI controller-based control. The M2 MOSFET delivers power to the load when the load exceeds what the grid and PV deliver. M1 MOSFET charges the battery when load is less than grid-plus-PV power.

3. RESULTS AND DISCUSSION

The simulation is developed for the PV connected grid system with EV and other loads connected. A controller defined in the previous section to improve power quality in the EV and nonlinear load connected PV-grid system is incorporated in the simulation. Specifications for the simulation are depicted in Table 1.

Power factor improvement and harmonic reduction with different configuration of loads are defined as cases. Four different load configurations are defined as cases and as defined in the following: i) linear load without controller, ii) linear load with controller, iii) non-linear load without controller, and iv) non-linear load with controller.

Since the EV gets involved in the system for the bidirectional power flow it is considered to be connected for all the cases. Results are observed for all the cases and discussed in this section. Grid voltage and current waveform depicting the bidirectional power flow due to loading variation is as shown in Figure 7. The complete graph Figure 7 for 1 sec shown and the zoomed view of AC side charging current and voltage is shown in Figure 7(a). Then Figure 7(b) shows the zoomed view of AC side discharging current and voltage.

Table 1. Specification of PV-EV-grid configuration

| Sl.no | Components | Ratings |
|-------|-----------------|---|
| 1 | PV array | $V_{mp} = 54.7 \text{ V}$, $V_{oc} = 64.2 \text{ V}$, $I_{mp} = 5.58 \text{ A}$, $I_{sc} = 5.96 \text{ A}$, No. of series connected panels=6 No. of parallel connected panels=48 |
| 2 | Grid | $V = 440 \text{ V}$ $F = 50 \text{ HZ}$ |
| 3 | Transformer | 1:1, 100 kVA, 50 HZ |
| 4 | Linear load | 80 kW |
| 5 | Non-linear load | Rectifier with $L=2 \text{ mH}$, $R=50\text{-}\Omega$, Wattage |
| 6 | Boost converter | $V_{out} = 700 \text{ V}$, $V_{in} = 300 \text{ V}$ |
| 7 | Inverter | 3-level, SVPWM |
| 8 | PHEV | 120 V li-ion battery with 50 Ah |

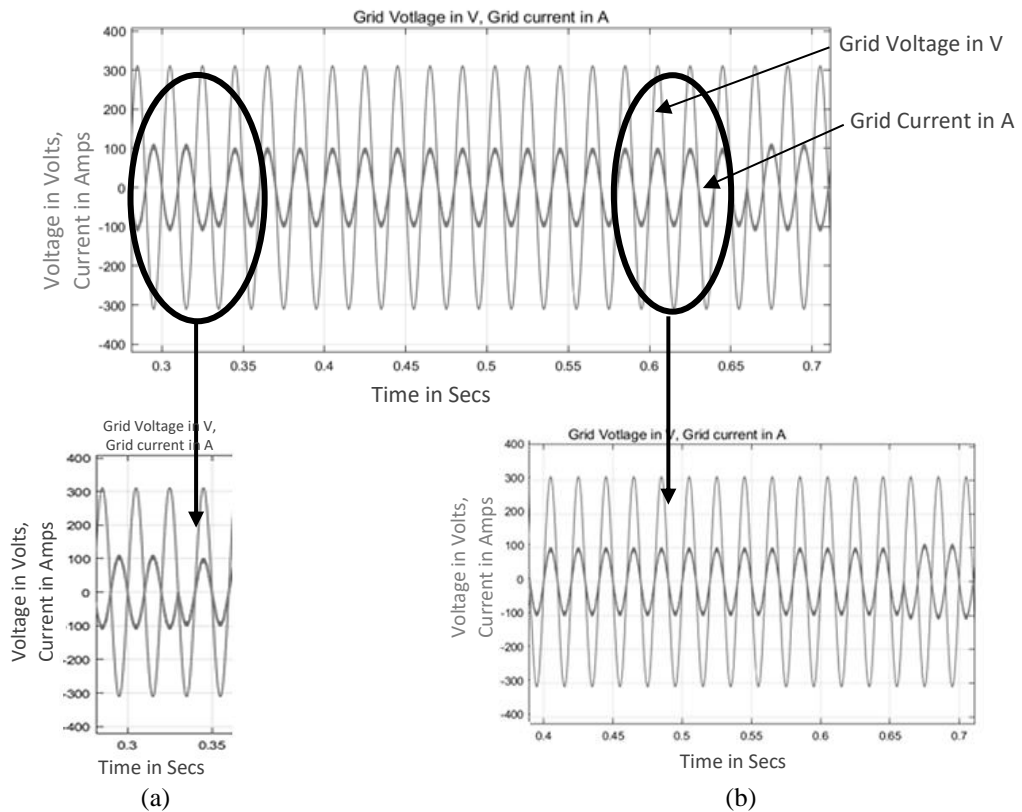


Figure 7. Voltage and current at PCC, (a) enlarged view when vehicle is charging and (b) enlarged view when vehicle is discharging

It can be observed that the direction of the current is from vehicle to the grid during the period of 0.33 to 0.66 seconds. While it is from the battery to the grid in other time period. The battery voltage and current waveform shown in Figure 8 also confirms this claim.

Charging (during 0 to 0.3 and 0.6 to 1 secs), discharging (during 0.3 to 0.6 secs) of the battery is controlled by the bidirectional controller given in Figure 7. Since constant current controller is used for the battery charging the 20 A is maintained constant both in charging and discharging mode. Low, medium, and high loading conditions are used for validation. Different loading conditions are defined as cases and results obtained are observed and discussed in this section. All the results are displayed in Table 2.

The power waveforms obtained from all three scenarios for the mentioned six cases are as given in the following. Three scenarios are implemented in the EV integration implementation in the PV integrated grid in the educational institution. The educational institution has a distribution transformer with a 100 kVA capacity. Linear load of maximum 80 kW. Analysis of power quality with and without the controllers is detailed. Scenario 1 (DQ controller), scenario 2 ($I\cos\phi$ controller) Scenario 3 (without controller) in the PV-EV-grid topology are discussed. In each scenario, six cases given in Table 2 are applied. The waveforms are compared with the conventional method developed in [12]. PV insolation is varied from 400 W/m² to 1,000 W/m² with 100 W/m² steps every 0.5 secs. The MPPT algorithm tracks the voltage, and maximum power tracking using the P and O algorithm is applied. The battery is discharged with the converter at 0.33 to 0.66 secs considering peak load. The battery is charged in two intervals 0 to 0.33 secs and 0.66 to 1 sec. This operation affects the waveforms of the DC link of the PHEV system. The battery voltage is high at the charging interval and low at discharging interval.

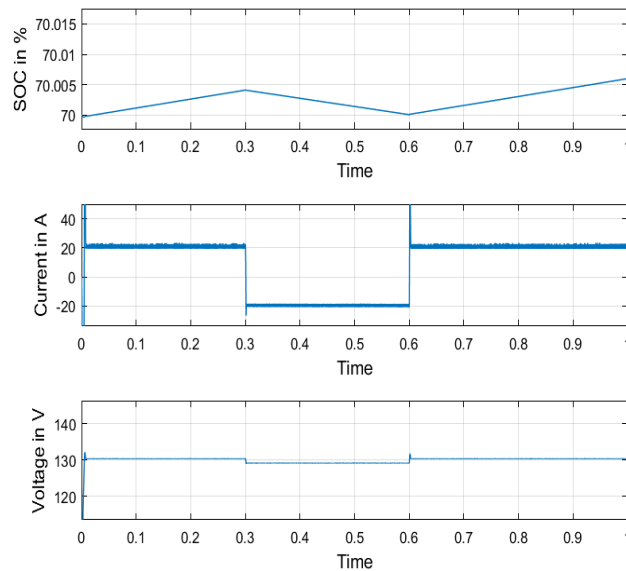


Figure 8. SOC, Battery voltage and battery current

Table 2. Different cases in proposed implementation

| Case Study | Loads in kW | | | Total |
|------------|-------------|------------|-----------|-------|
| | Linear | Non-linear | PHEV load | |
| C 1 | 0 | 8.8 | 6.6 | 15.4 |
| C 2 | 8.8 | 0 | 6.6 | 15.4 |
| C 3 | 50 | 0 | 6.6 | 56.6 |
| C 4 | 0 | 50 | 6.6 | 56.6 |
| C 5 | 80 | 0 | 6.6 | 86.6 |
| C 6 | 0 | 80 | 6.6 | 86.6 |

Power response at load, PCC and PV inverter output in the PV-EV-grid topology with controller for DQ controller all six-loading condition in Table 2 is as shown in Figure 9. Figure 9 is grouped with all the six cases in single figure to make the comparison easy. The scenario 1 with all the cases respectively is grouped. Figure 9(a) shows the case 1, Figure 9(b) shows the case 2, Figure 9(c) shows the case 3, Figure 9(d) shows the case 4, Figure 9(e) shows the case 5 and Figure 9(f) shows the case 6. In scenario 1 in all the cases shows the achievement of balancing of power. And Figure 10 shows the scenario 2 with Figure 10(a) case 1 (C1), Figure 10(b) case 2 (C2), Figure 10(c) case 3 (C3), Figure 10(d) case 4 (C4), Figure 10(e) case 5 (C5) and Figure 10(f) case 6 (C6) grouped respectively. In scenario 2 also in all the cases it shows the power balancing

of power. The power response of PV given in the equations is seen to be stepped due to insolation variation at every 0.1 seconds. Load power and PCC power waveform follows the battery charging/discharging pattern. The excess in PV power supplies to the grid PCC thus showing the power curve direction to be negative.

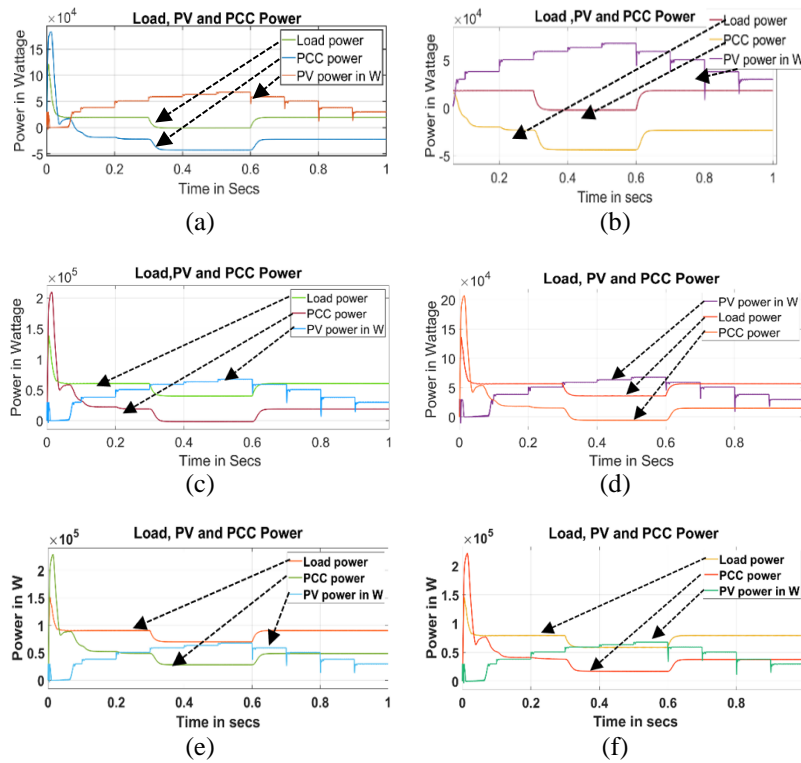


Figure 9. Scenario 1 (a) C1, (b) C2, (c) C3, (d) C4, (e) C5, and (f) C6

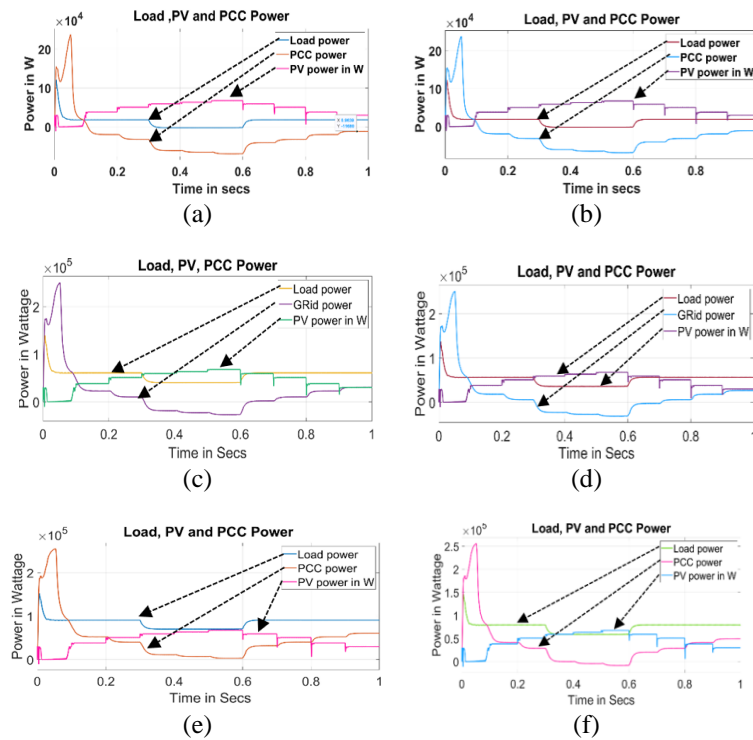


Figure 10. Scenario 2 (a) C1, (b) C2, (c) C3, (d) C4, (e) C5, and (f) C6

Since THD is a primary criterion for power quality measurements in the grid-connected system, it is tabulated for all three scenarios in Table 3. Observation of THD from all three scenarios infers that harmonic mitigation capability with the DQ controller is found to be dominating between the two controllers involved. Table 4 shows significant improvement in THD compared with the conventional method. Observation from both $I\cos\phi$ and composite controller (with DQ controller) is tabulated as given in Table 4. A significant improvement in harmonic reduction is observed while calculating the percentage improvement in the THD using the composite controller (with DQ controller) compared to the $I\cos\phi$ method. The power quality performance thus obtained by the composite controller (with DQ controller) with has outperformed the $I\cos\phi$ controller while maintaining a healthy charging and discharging cycle in the controller.

Table 3. THD in Scenario 1, 2 and 3

| Scenario 1 | Voltage THD | Current THD |
|------------|-------------|-------------|
| C1 | 3.32% | 1.61% |
| C2 | 2.88% | 1.55% |
| C3 | 1.20% | 3.30% |
| C4 | 3.28% | 11.84% |
| C5 | 0.82% | 1.27% |
| C6 | 3.26% | 6.30% |
| Scenario2 | Voltage THD | Current THD |
| C1 | 2.61% | 1.14% |
| C2 | 1.86% | 0.97% |
| C3 | 0.56% | 2.25% |
| C4 | 2.29% | 3.20% |
| C5 | 0.40% | 0.78% |
| C6 | 2.34% | 5.85% |
| Scenario3 | Voltage THD | Current THD |
| C1 | 3.20% | 74.37% |
| C2 | 2.09% | 4.92% |
| C3 | 1.14% | 0.82% |
| C4 | 3.18% | 31.56% |
| C5 | 0.77% | 0.36% |
| C6 | 3.19% | 29.07% |

Table 4. Percentage improvement in THD compared with scenario 1 and scenario 2

| DQ controller current THD in % | $I\cos\phi$ controller current THD in % | % Improvement of THD |
|--------------------------------|---|----------------------|
| 1.14% | 1.61% | 29.19% |
| 0.97% | 1.55% | 37.42% |
| 2.25% | 3.30% | 31.82% |
| 3.20% | 11.84% | 72.97% |
| 0.78% | 1.27% | 38.58% |
| 5.85% | 6.30% | 7.14% |

4. CONCLUSION

The proposed controller topology with three-phase inverters and a combined controller (with DQ controller) is designed in MATLAB Software. The proposed controller performance out performs the traditional $I\cos\phi$ controller in the power quality performance. The THD of the proposed controller is well within the IEEE 519 standards in all six cases. Decoupling the bidirectional controller and the grid synchronization controller is advantageous in the EV-PV-grid scenarios. The PV power plant with the power quality conditioning is done using the 3-level inverter. The comparison of THD observes domination by the proposed controller. The proposed control technique is multicarrier SVPWM, which controls the 3-level inverter and has outperformed the $I\cos\phi$ controller. The THD is reduced compared to the $I\cos\phi$ presented if replaced with a DQ controller. In future, the single-phase charge controllers can be replaced with three-phase.

REFERENCES




- [1] K. Clement-nyns, K. Van Reusel, and J. Driesen, "The consumption of electrical energy of plug-in hybrid electric vehicles in Belgium," in *EET-2007 European Ele-Drive Conference*, 2007.
- [2] L. P. Fernandez, T. G. S. Roman, R. Cossent, C. M. Domingo, and P. Frias, "Assessment of the impact of plug-in electric vehicles on distribution networks," *IEEE Transactions on Power Systems*, vol. 26, no. 1, pp. 206–213, Feb. 2011, doi: 10.1109/TPWRS.2010.2049133.
- [3] P. M. de Quevedo, G. Munoz-Delgado, and J. Contreras, "Impact of electric vehicles on the expansion planning of distribution systems considering renewable energy, storage, and charging stations," *IEEE Transactions on Smart Grid*, vol. 10, no. 1, pp. 794–804, Jan. 2019, doi: 10.1109/TSG.2017.2752303.

- [4] M. Zeraati, M. E. H. Golshan, and J. M. Guerrero, "A consensus-based cooperative control of PEV battery and PV active power curtailment for voltage regulation in distribution networks," *IEEE Transactions on Smart Grid*, vol. 10, no. 1, pp. 670–680, Jan. 2019, doi: 10.1109/TSG.2017.2749623.
- [5] Z. Akhtar, M. Opatovsky, B. Chaudhuri, and S. Y. R. Hui, "Comparison of point-of-load versus mid-feeder compensation in LV distribution networks with high penetration of solar photovoltaic generation and electric vehicle charging stations," *IET Smart Grid*, vol. 2, no. 2, pp. 283–292, Jun. 2019, doi: 10.1049/iet-stg.2018.0193.
- [6] J. Wang, G. R. Bharati, S. Paudyal, O. Ceylan, B. P. Bhattarai, and K. S. Myers, "Coordinated electric vehicle charging with reactive power support to distribution grids," *IEEE Transactions on Industrial Informatics*, vol. 15, no. 1, pp. 54–63, Jan. 2019, doi: 10.1109/II.2018.2829710.
- [7] S. Faddel and O. Mohammed, "Automated distributed electric vehicle controller for residential demand side management," in *2017 IEEE Industry Applications Society Annual Meeting*, Oct. 2017, pp. 1–8, doi: 10.1109/IAS.2017.8101709.
- [8] J. Gupta, R. Maurya, and S. R. Arya, "Improved power quality on-board integrated charger with reduced switching stress," *IEEE Transactions on Power Electronics*, vol. 35, no. 10, pp. 10810–10820, Oct. 2020, doi: 10.1109/TPEL.2020.2981955.
- [9] B. Singh and R. Kushwaha, "EV battery charger with non-inverting output voltage-based bridgeless PFC Cuk converter," *IET Power Electronics*, vol. 12, no. 13, pp. 3359–3368, Nov. 2019, doi: 10.1049/iet-pel.2019.0037.
- [10] R. Kushwaha and B. Singh, "Interleaved landsman converter fed EV battery charger with power factor correction," in *2018 IEEE 8th Power India International Conference (PIICON)*, Dec. 2018, pp. 1–6, doi: 10.1109/POWERI.2018.8704418.
- [11] A. K. Verma, B. Singh, D. T. Shahani, and C. Jain, "Grid-interfaced solar photovoltaic smart building with bidirectional power flow between grid and electric vehicle with improved power quality," *Electric Power Components and Systems*, vol. 44, no. 5, pp. 480–494, Mar. 2016, doi: 10.1080/15325008.2015.1120818.
- [12] N. B. G. Brinkel *et al.*, "Impact of rapid PV fluctuations on power quality in the low-voltage grid and mitigation strategies using electric vehicles," *International Journal of Electrical Power and Energy Systems*, vol. 118, Jun. 2020, doi: 10.1016/j.ijepes.2019.105741.
- [13] V. A. Katic, A. M. Stanisavljevic, B. P. Dumnic, and B. P. Popadic, "Impact of V2G operation of electric vehicle chargers on distribution grid during voltage dips," in *IEEE EUROCON 2019-18th International Conference on Smart Technologies*, Jul. 2019, pp. 1–6, doi: 10.1109/EUROCON.2019.8861904.
- [14] S. Chaurasiya and B. Singh, "A G2V/V2G off-board fast charger for charging of lithium-ion based electric vehicles," in *2019 IEEE International Conference on Environment and Electrical Engineering and 2019 IEEE Industrial and Commercial Power Systems Europe (EEEIC/I and CPS Europe)*, Jun. 2019, pp. 1–6, doi: 10.1109/EEEIC.2019.8783305.
- [15] X. Chen, Q. Fu, S. Yu, and L. Zhou, "Unified control of photovoltaic grid-connection and power quality managements," in *2008 Workshop on Power Electronics and Intelligent Transportation System*, Aug. 2008, pp. 360–365, doi: 10.1109/PEITS.2008.66.
- [16] H. F. Farahani, "Improving voltage unbalance of low-voltage distribution networks using plug-in electric vehicles," *Journal of Cleaner Production*, vol. 148, pp. 336–346, Apr. 2017, doi: 10.1016/j.jclepro.2017.01.178.
- [17] F. Geth, N. Leemput, J. Van Roy, J. Buscher, R. Ponnente, and J. Driesen, "Voltage droop charging of electric vehicles in a residential distribution feeder," in *2012 3rd IEEE PES Innovative Smart Grid Technologies Europe (ISGT Europe)*, Oct. 2012, pp. 1–8, doi: 10.1109/ISGTEurope.2012.6465692.
- [18] S. Huang, J. R. Pillai, B. Bak-Jensen, and P. Thogersen, "Voltage support from electric vehicles in distribution grid," in *2013 15th European Conference on Power Electronics and Applications (EPE)*, Sep. 2013, pp. 1–8, doi: 10.1109/EPE.2013.6634344.
- [19] A. Supponen, A. Rautiainen, J. Markkula, A. Mäkinen, P. Jarventausta, and S. Repo, "Power quality in distribution networks with electric vehicle charging—a research methodology based on field tests and real data," in *2016 Eleventh International Conference on Ecological Vehicles and Renewable Energies (EVER)*, Apr. 2016, pp. 1–11, doi: 10.1109/EVER.2016.7476376.
- [20] M. Jayachandran, K. P. Rao, R. K. Gatla, C. Kalaiivani, C. Kalaiarasy, and C. Logasabarirajan, "Operational concerns and solutions in smart electricity distribution systems," *Utilities Policy*, vol. 74, Feb. 2022, doi: 10.1016/j.jup.2021.101329.
- [21] A. Lucas, F. Bonavitacola, E. Kotsakis, and G. Fulli, "Grid harmonic impact of multiple electric vehicle fast charging," *Electric Power Systems Research*, vol. 127, pp. 13–21, Oct. 2015, doi: 10.1016/j.epr.2015.05.012.
- [22] A. Rautiainen *et al.*, "Case studies on impacts of plug-in vehicle charging load on the planning of urban electricity distribution networks," in *2013 Eighth International Conference and Exhibition on Ecological Vehicles and Renewable Energies (EVER)*, Mar. 2013, pp. 1–7, doi: 10.1109/EVER.2013.6521542.
- [23] M. Bollen and F. Hassan, *Integration of distributed generation in the power system*. Hoboken, NJ, USA: John Wiley and Sons, Inc., 2011, doi: 10.1002/9781118029039.
- [24] J. C. Ferreira, V. Monteiro, J. L. Afonso, and A. Silva, "Smart electric vehicle charging system," in *2011 IEEE Intelligent Vehicles Symposium (IV)*, Jun. 2011, pp. 758–763, doi: 10.1109/IVS.2011.5940579.
- [25] J. C. Gomez and M. M. Morcos, "Impact of EV battery chargers on the power quality of distribution systems," *IEEE Transactions on Power Delivery*, vol. 18, no. 3, pp. 975–981, Jul. 2003, doi: 10.1109/TPWRD.2003.813873.
- [26] Y. Du, S. Lukic, B. Jacobson, and A. Huang, "Review of high power isolated bi-directional DC-DC converters for PHEV/EV DC charging infrastructure," in *2011 IEEE Energy Conversion Congress and Exposition*, Sep. 2011, pp. 553–560, doi: 10.1109/ECCE.2011.6063818.
- [27] W. Shireen and S. Patel, "Plug-in hybrid electric vehicles in the smart grid environment," in *IEEE PES T and D 2010*, 2010, pp. 1–4, doi: 10.1109/TDC.2010.5484254.
- [28] X. Zhou, S. Lukic, S. Bhattacharya, and A. Huang, "Design and control of grid-connected converter in bi-directional battery charger for plug-in hybrid electric vehicle application," in *2009 IEEE Vehicle Power and Propulsion Conference*, Sep. 2009, pp. 1716–1721, doi: 10.1109/VPPC.2009.5289691.
- [29] K. Clement-Nyns, E. Haesen, and J. Driesen, "The impact of charging plug-in hybrid electric vehicles on a residential distribution grid," *IEEE Transactions on Power Systems*, vol. 25, no. 1, pp. 371–380, Feb. 2010, doi: 10.1109/TPWRS.2009.2036481.
- [30] C. A. Hill, M. C. Such, D. Chen, J. Gonzalez, and W. M. Grady, "Battery energy storage for enabling integration of distributed solar power generation," *IEEE Transactions on Smart Grid*, vol. 3, no. 2, pp. 850–857, Jun. 2012, doi: 10.1109/TSG.2012.2190113.
- [31] N. Shaukat *et al.*, "A survey on electric vehicle transportation within smart grid system," *Renewable and Sustainable Energy Reviews*, vol. 81, pp. 1329–1349, Jan. 2018, doi: 10.1016/j.rser.2017.05.092.
- [32] C. Pang, P. Dutta, and M. Kezunovic, "BEVs/PHEVs as dispersed energy storage for V2B uses in the smart grid," *IEEE Transactions on Smart Grid*, vol. 3, no. 1, pp. 473–482, Mar. 2012, doi: 10.1109/TSG.2011.2172228.
- [33] Y. Gurkaynak and A. Khaligh, "Control and power management of a grid connected residential photovoltaic system with plug-in hybrid electric vehicle (PHEV) load," in *2009 Twenty-Fourth Annual IEEE Applied Power Electronics Conference and Exposition*, Feb. 2009, pp. 2086–2091, doi: 10.1109/APEC.2009.4802962.
- [34] M. Karimi-Ghartemani and A. K. Ziarani, "A nonlinear time-frequency analysis method," *IEEE Transactions on Signal Processing*, vol. 52, no. 6, pp. 1585–1595, Jun. 2004, doi: 10.1109/TSP.2004.827155.




- [35] B. Singh, S. S. Murthy, and S. Gupta, "Analysis and design of STATCOM-based voltage regulator for self-excited induction generators," *IEEE Transactions on Energy Conversion*, vol. 19, no. 4, pp. 783–790, Dec. 2004, doi: 10.1109/TEC.2004.827710.
- [36] Z. Hekss *et al.*, "Advanced nonlinear controller of single-phase shunt active power filter interfacing solar photovoltaic source and electrical power grid," *International Transactions on Electrical Energy Systems*, vol. 31, no. 12, Dec. 2021, doi: 10.1002/2050-7038.13237.
- [37] A. Ziarani and A. Konrad, "A method of extraction of nonstationary sinusoids," *Signal Processing*, vol. 84, no. 8, pp. 1323–1346, Aug. 2004, doi: 10.1016/j.sigpro.2004.05.008.
- [38] P. Jintakosonwit, H. Fujita, H. Akagi, and S. Ogasawara, "Implementation and performance of cooperative control of shunt active filters for harmonic damping throughout a power distribution system," *IEEE Transactions on Industry Applications*, vol. 39, no. 2, pp. 556–564, Mar. 2003, doi: 10.1109/TIA.2003.808959.
- [39] J. G. Pinto, R. Pregitzer, L. F. C. Monteiro, and J. L. Afonso, "3-phase 4-wire shunt active power filter with renewable energy interface," *Renewable Energy and Power Quality Journal*, vol. 1, no. 05, pp. 625–630, Mar. 2007, doi: 10.24084/repqj05.350.
- [40] J. M. Carrasco *et al.*, "Power-electronic systems for the grid integration of renewable energy sources: A survey," *IEEE Transactions on Industrial Electronics*, vol. 53, no. 4, pp. 1002–1016, Jun. 2006, doi: 10.1109/TIE.2006.878356.
- [41] M. Elshaer, A. Mohamed, and O. Mohammed, "Smart optimal control of DC-DC boost converter in PV systems," in *2010 IEEE/PES Transmission and Distribution Conference and Exposition: Latin America (T and D-LA)*, Nov. 2010, pp. 403–410, doi: 10.1109/TDC-LA.2010.5762913.
- [42] Z. Ibrahim, A. shukri A. Hasim, M. H. N. Talib, J. M. Lazi, S. N. B. M. Isa, and R. Mustafa, "Performance investigation of photovoltaic grid connection for shunt active power filter with different PWM generation," *Journal of Theoretical and Applied Information Technology*, vol. 57, no. 2, pp. 305–312, 2013.
- [43] D. Wang, K. Meng, X. Gao, J. Qiu, L. L. Lai, and Z. Y. Dong, "Coordinated dispatch of virtual energy storage systems in LV grids for voltage regulation," *IEEE Transactions on Industrial Informatics*, vol. 14, no. 6, pp. 2452–2462, Jun. 2018, doi: 10.1109/TII.2017.2769452.

BIOGRAPHIES OF AUTHORS



Basaralu Nagasiddalingaiah Harish    is an Asst Professor in the Electrical and Electronics Engineering Department, PES College of Engineering, Mandya, Karnataka. He completed his B.E in Electrical and Electronics Engineering from KVG College of Engineering, Sullia, Karnataka, India in 2000, M.Tech in Computer Applications in Industrial drives 2004 from the National Institute of Engineering, Mysore, India and pursuing a Ph.D in CHRIST (Deemed to be University) Bangalore, India. He has 15 years of teaching experience. He is an IEEE Member. His research interest includes power electronics, drives, control system, flexible AC transmission system. He can be contacted at email: bn.harish@res.christuniversity.in.



Usha Surendra    Professor in Electrical and Electronics Engineering Department, School of Engineering and Technology, CHRIST (Deemed to be University), Bangalore, has completed her Ph.D. in Electronics, PET Research Centre, the University of Mysore during 2013. She has 10 years of industrial experience and 27 years of academic knowledge. She has published 08 international journals, authored 2 book chapters, and was involved in research activity, including high voltage engineering and renewable engineering. She can be contacted at email: usha.surendra@christuniversity.in.